Modeling the impact of high and thermal energy neutron flux on semiconductor film heterostructures

V.R.Yamurzin, engineer FL’nP
Scientific Supervisor: Head of Sector, Ph.D. in Physics and Mathematics, M.V.Bulavin
Joint Institute for Nuclear Research (JINR),
E-mail: yamurzin.v@nf.jinr.ru

Introduction

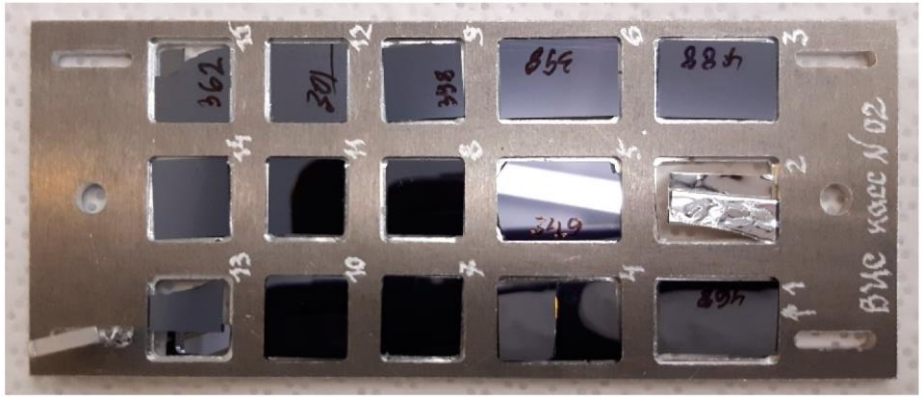

Photograph of a cassette holder with several heterostructures.

the fixtures allocation on th supporting beam in the channel #3 of the IBR-2 reactor

Basic material parameters

The targets used were models of InAs material with various thicknesses ranging to 1 cm with the following parameters: Density 5.670 g/cm3, radiation length: 1.741 cm, nuclear interaction length: 28.273 cm, Imean (mean ionization energy): 424.674 eV, Temperature: 293.15 K, pressure 1.00 atm.

Table of isotopes and abundances of elements in the target material

Element	N	ElmMassFraction, %	Abundance, %	ElmAbundance, %
In	113	60	5	49.46
	115		95	
As	75	40	100	50.54

Basic material parameters

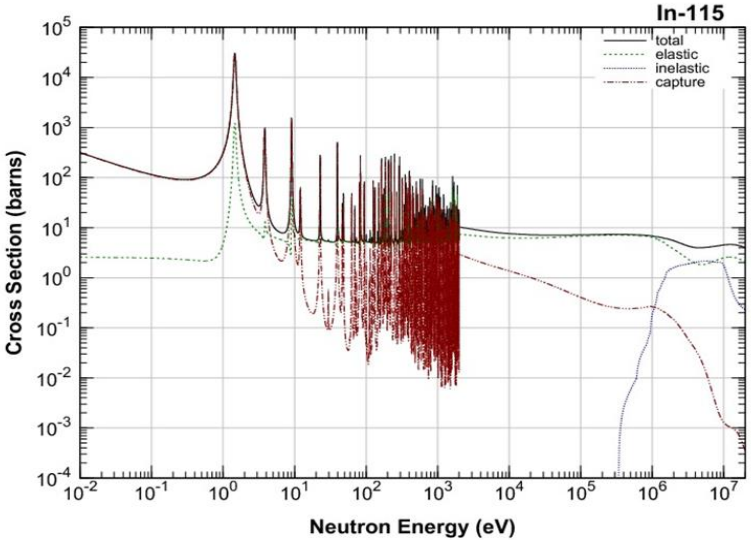

Reaction cross sections for In^{115}

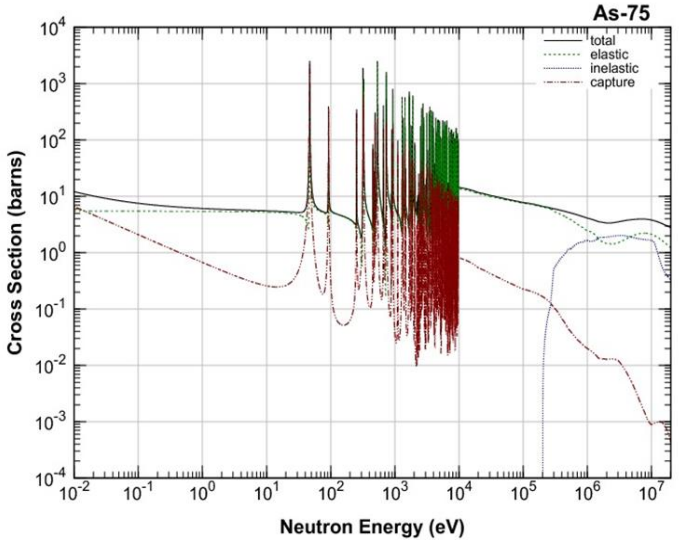

Reaction cross sections for As^{75}

Simulation parameters

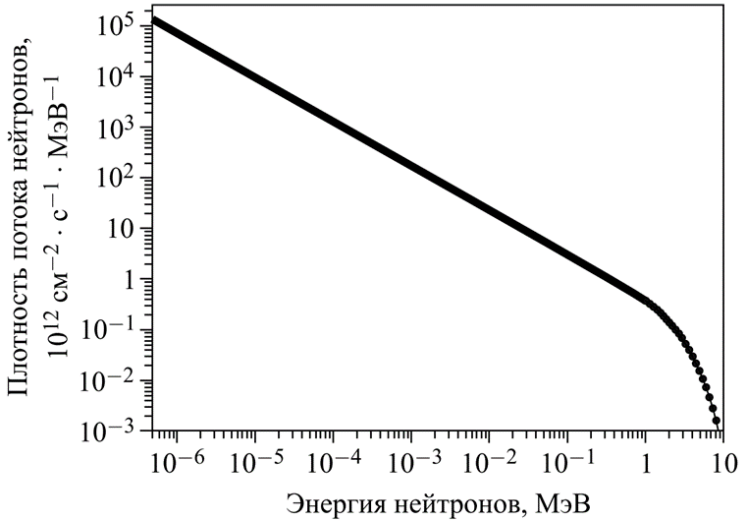

Differential energy density of neutron flux in channel No. 3 of the IBR-2 reactor at a distance of 0.3 m from the water moderator

Modeling was conducted for both monoenergetic neutrons with energies of 0.0253 eV and 14 MeV, as well as for the neutron spectrum. The experimental energy spectrum of neutrons from the IBR-2 reactor channel #3 at a distance of 30 mm from the water moderator was used as the energy spectrum. The main reactions important for our analysis are:

- **Elastic** scattering
- **Inelastic** scattering
- **nCapture** (neutron capture)

Geant results

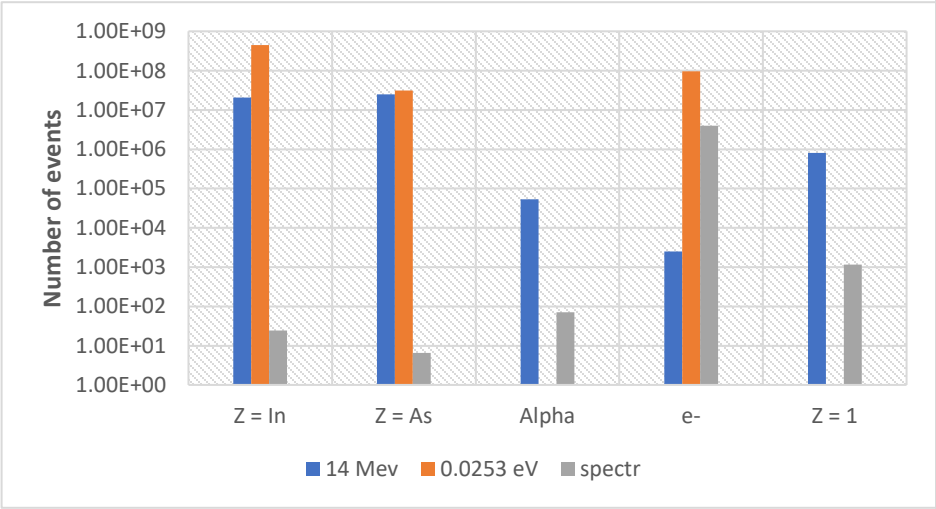

The calculated number of secondary particles formed after the interaction of neutrons of various energies with the nuclei of the crystal lattice of the material

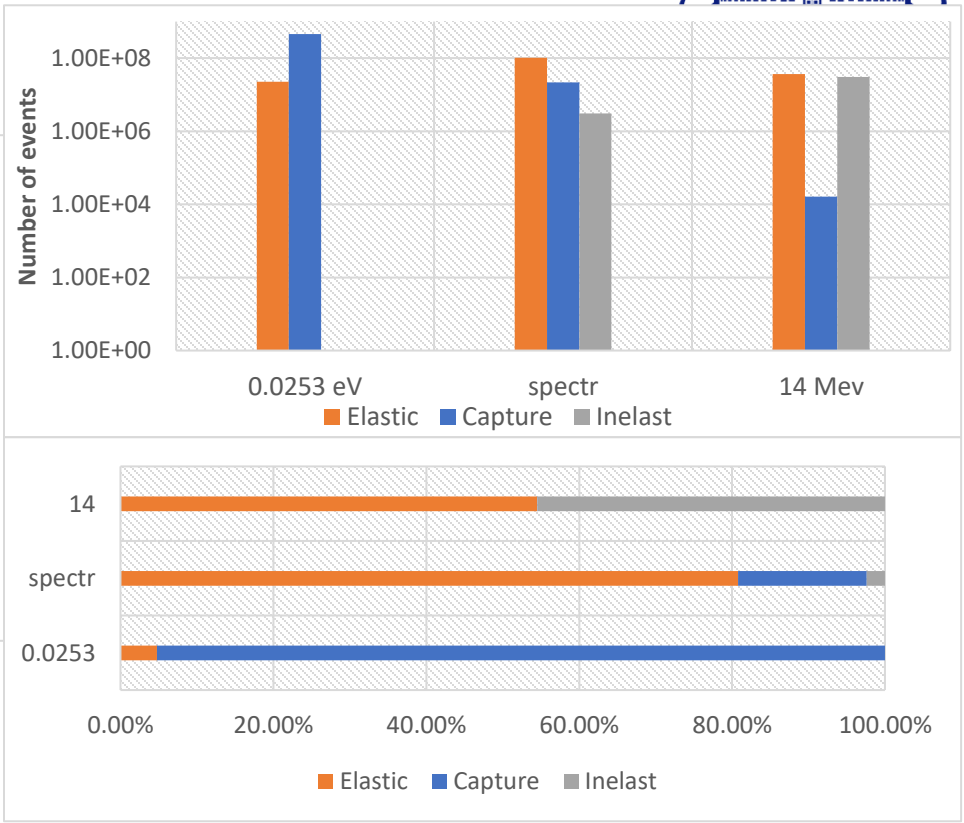

Calculated fraction of elastic, inelastic events and capture reactions for various neutron radiation energies

Geant results

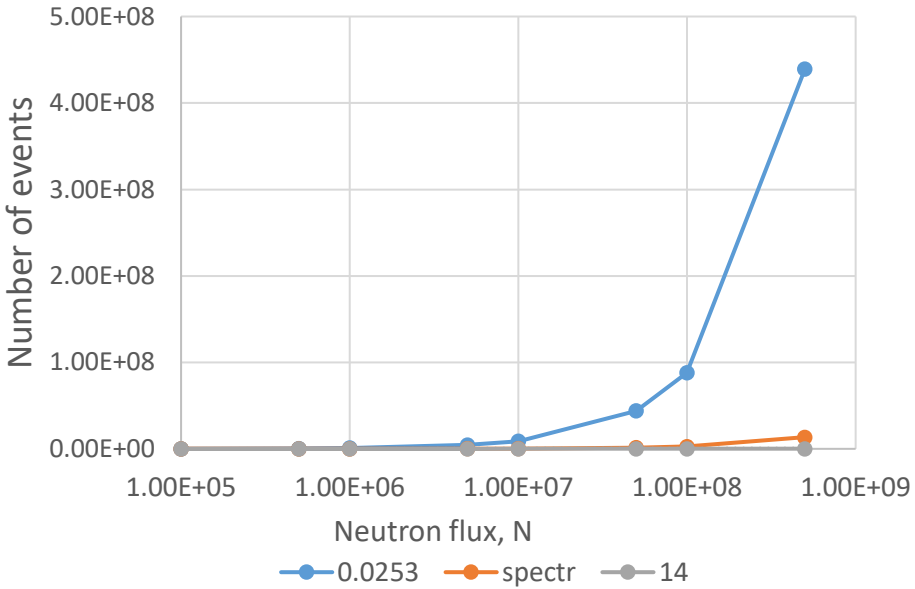

Dependence of the resulting free charge carriers on the neutron flux

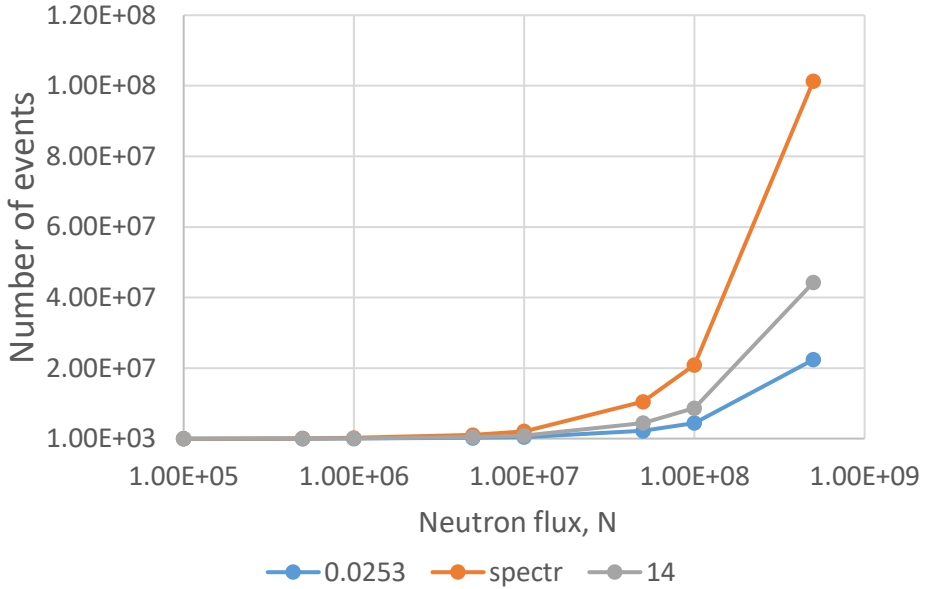

Dependence of formed defects on neutron flux

SRIM results

Linear transfer of energy (LET) and range of charged particles inside InAs depending on energy

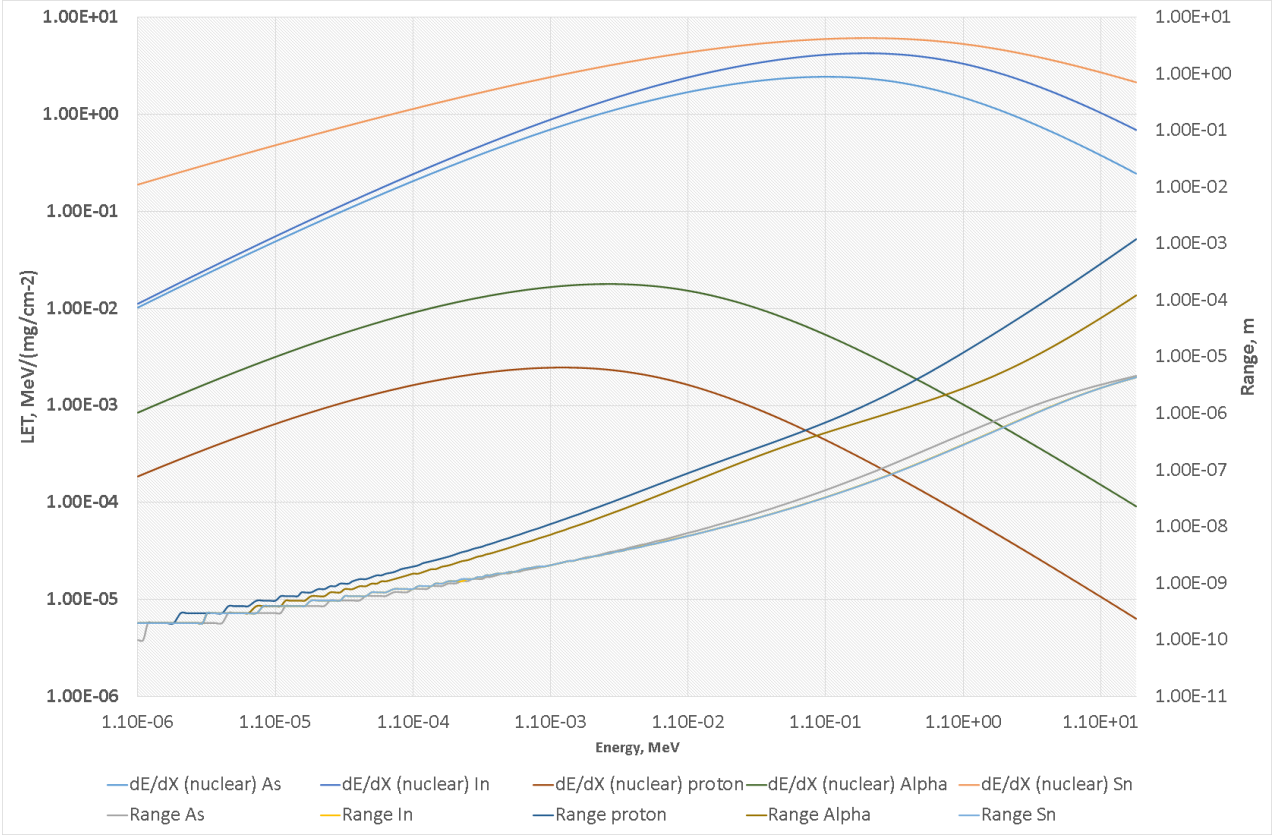

Conclusion

The results obtained allow us to better understand the processes, the formation of a crystal in the lattice of this material and its stability at different neutron energies.

These advanced analysis techniques allow us to enhance the effect of neutron flux on semiconductors, clarifying the dynamics of sound under different conditions. Particular attention is paid to the influence of both fast and thermal neutrons on the formation of defects and final charge carriers, which contributes to the creation of more accurate models of the behavior of semiconductor materials under the influence of various types of neutrons.

PHEMT

Composition	Layer	Width, nm	Doping
i-GaAs	Cap	9	-
$Al_{0.24}Ga_{1-x}As$	Barrier	25	-
δ—Si	Doping	-	$N_D = 5 \cdot 10^{12}$ см$^{-2}$
$Al_{0.24}Ga_{1-x}As$	Spacer	5	-
$In_{0.21}Ga_{1-Y}As$	Channel	11	-
GaAs	Buffer	400	-
GaAs	Substrate	350 μm	-

InP HEMT

Composition	Layer	Width, nm	Doping
$In_{0.53}Ga_{0.47}As$	Cap	9	-
$In_{0.52}Al_{0.48}As$	Barrier	25	-
δ—Si	Doping	-	$N_D = 5 \cdot 10^{12}$ см$^{-2}$
$In_{0.52}Al_{0.48}As$	Spacer	5	-
$In_{0.53}Ga_{0.47}As$	Channel	11	-
$In_{0.52}Al_{0.48}As$	Buffer	350	-
InP	Substrate	350 μm	-

MHEMT

Composition	Layer	Width, nm	Doping
$In_{0.53}Ga_{0.47}As$	Cap	9	-
$In_{0.52}Al_{0.48}As$	Barrier	25	-
δ—Si	Doping	-	$N_D = 5 \cdot 10^{12}$ см$^{-2}$
$In_{0.52}Al_{0.48}As$	Spacer	5	-
$In_{0.53}Ga_{0.47}As$	Channel	11	-
$In_{0.52}Al_{0.48}As$	Smoothing layer	180	-
$In_{0.55}Al_{0.45}As$	Inverse step	30	--
$In_xAl_{1-x}As$ (x= 0.1, 0.2, 0.3, 0.4, 0.52)	Step graded MB (5 layers)	5 x 200 nm	-
GaAs	Buffer	100	
GaAs	Substrate	350 μm	

Thank you for your attention

Оптические свойства

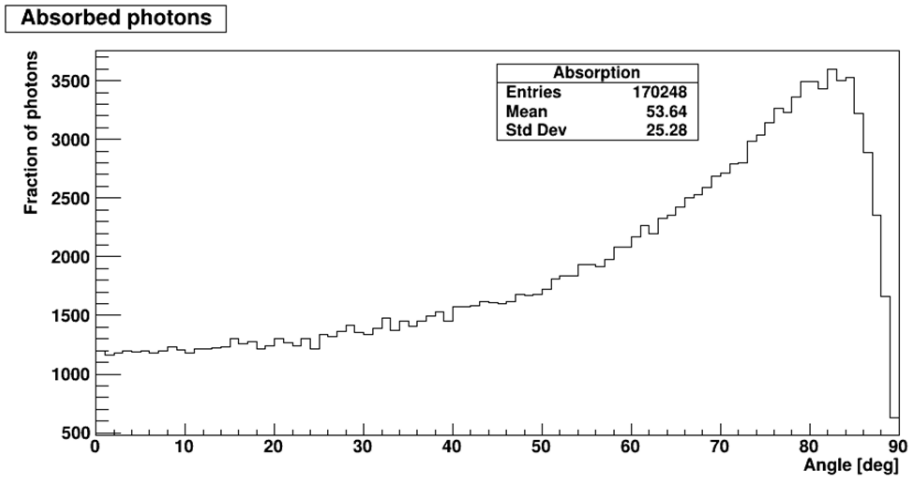

Доля поглощённых материалом фотонов до облучения

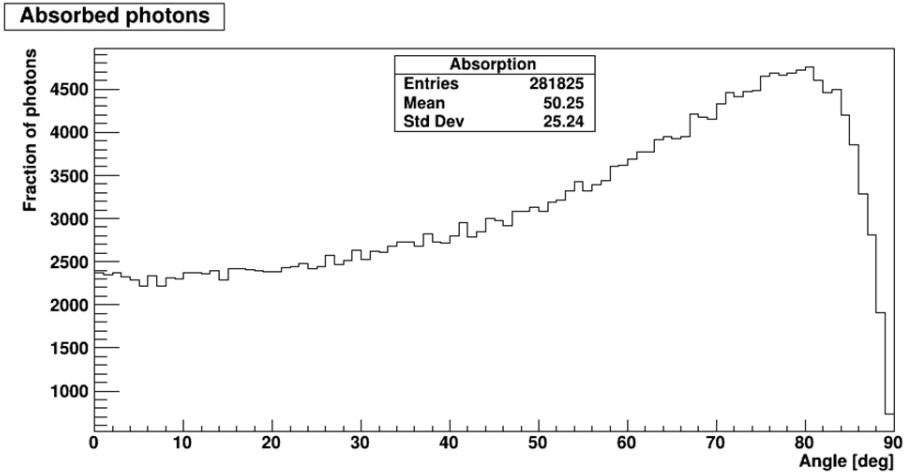

Доля поглощённых материалом фотонов после облучения

Результаты

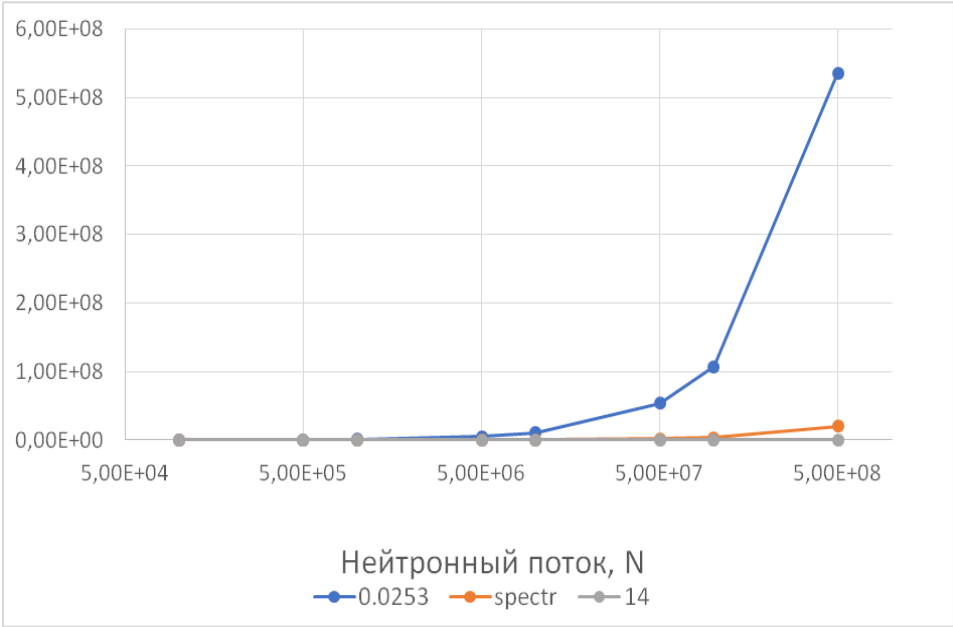

Зависимость образовавшихся свободных носителей заряда относительно нейтронного потока

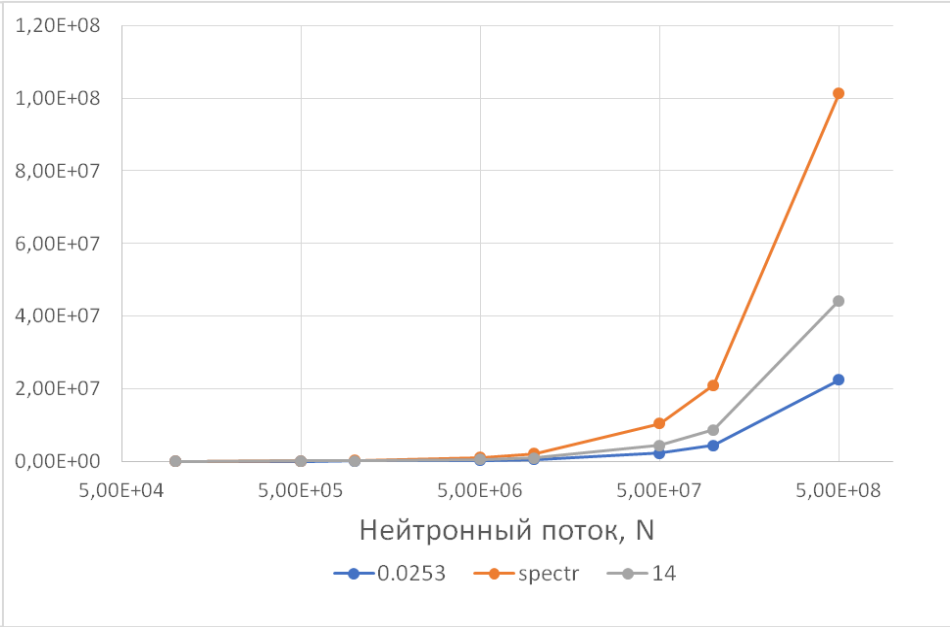

Зависимость образовавшихся дефектов относительно нейтронного потока

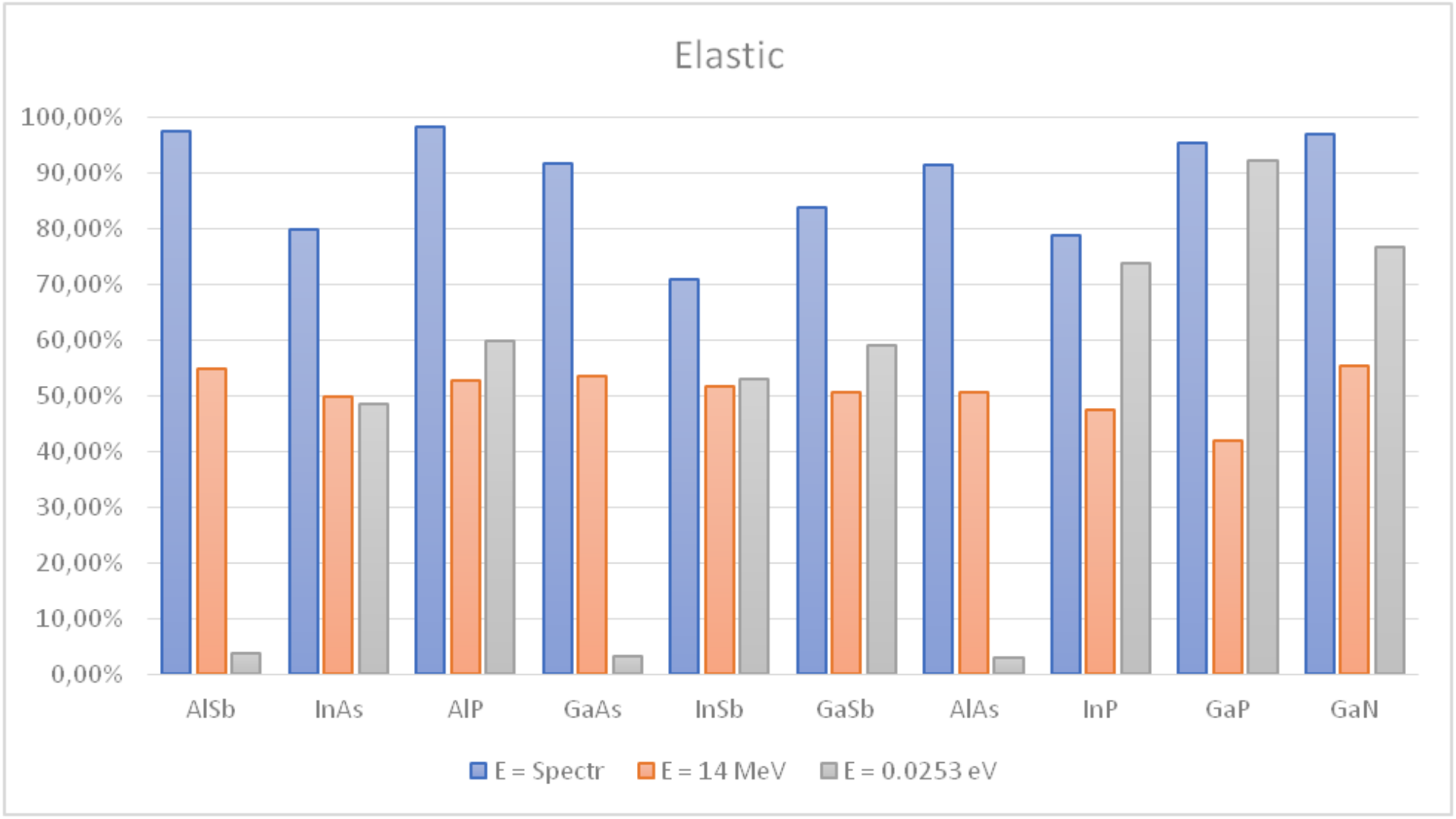
Elastic
100,00%
90,00%
80,00%
70,00%
60,00%
50,00%
40,00%
30,00%
20,00%
10,00%
0,00%
AlSb
InAs
AlP
GaAs
InSb
GaSb
AlAs
InP
GaP
GaN
E = Spectr
E = 14 MeV
E = 0.0253 eV

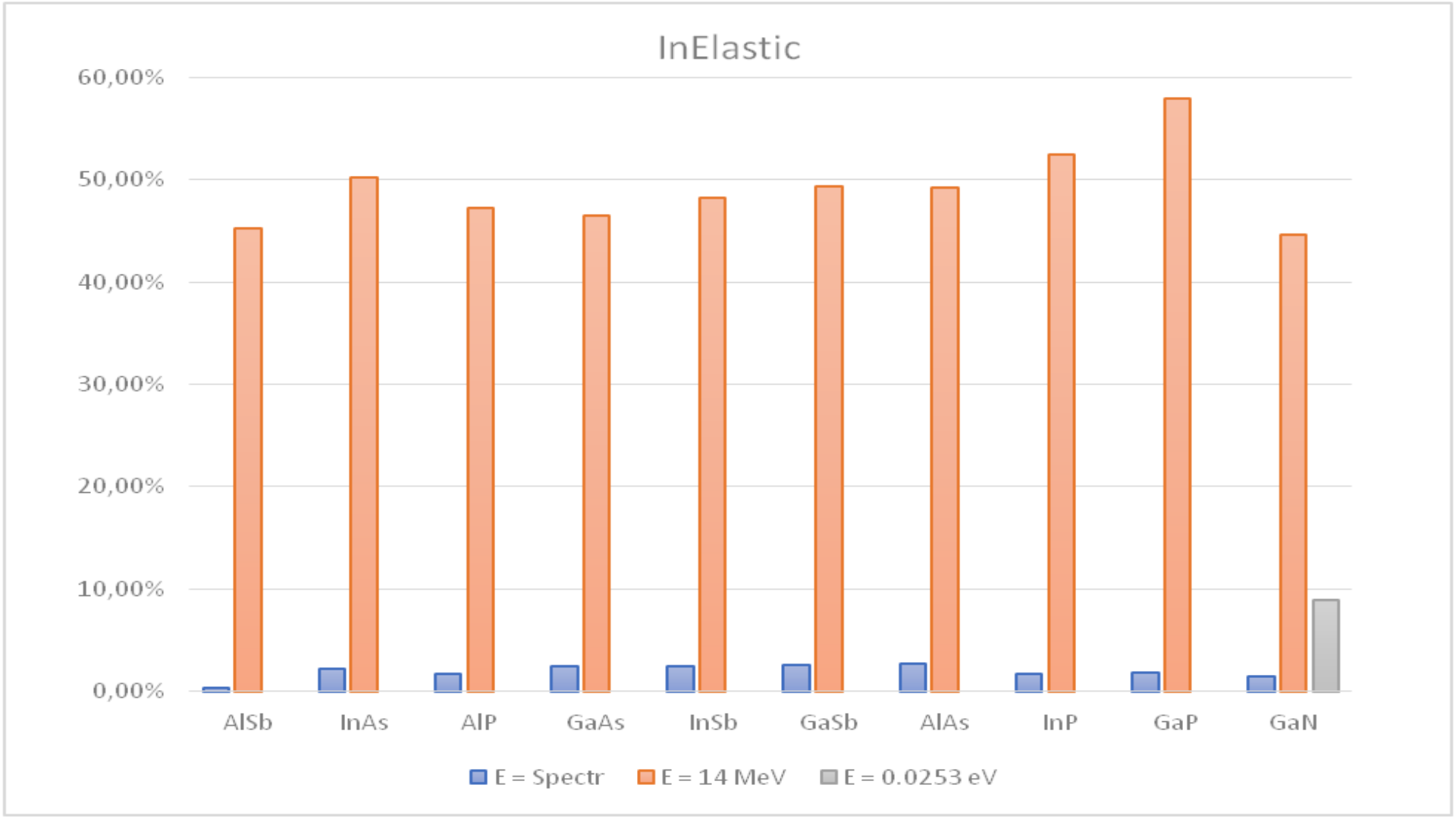
InElastic
60,00%
50,00%
40,00%
30,00%
20,00%
10,00%
0,00%
AlSb
InAs
AlP
GaAs
InSb
GaSb
AlAs
InP
GaP
GaN
E = Spectr
E = 14 MeV
E = 0.0253 eV

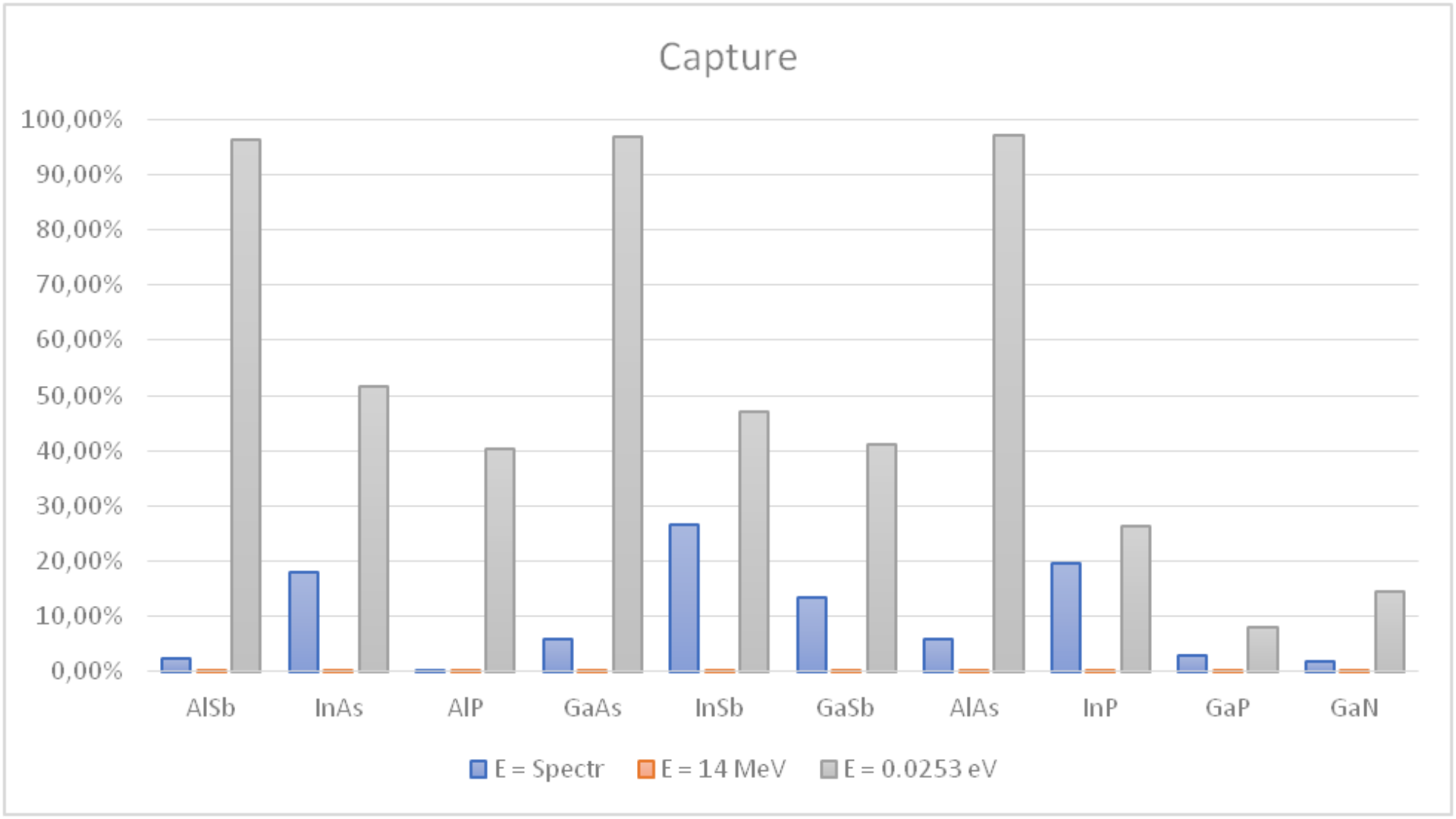
Capture
100,00%
90,00%
80,00%
70,00%
60,00%
50,00%
40,00%
30,00%
20,00%
10,00%
0,00%
AlSb
InAs
AlP
GaAs
InSb
GaSb
AlAs
InP
GaP
GaN
E = Spectr
E = 14 MeV
E = 0.0253 eV

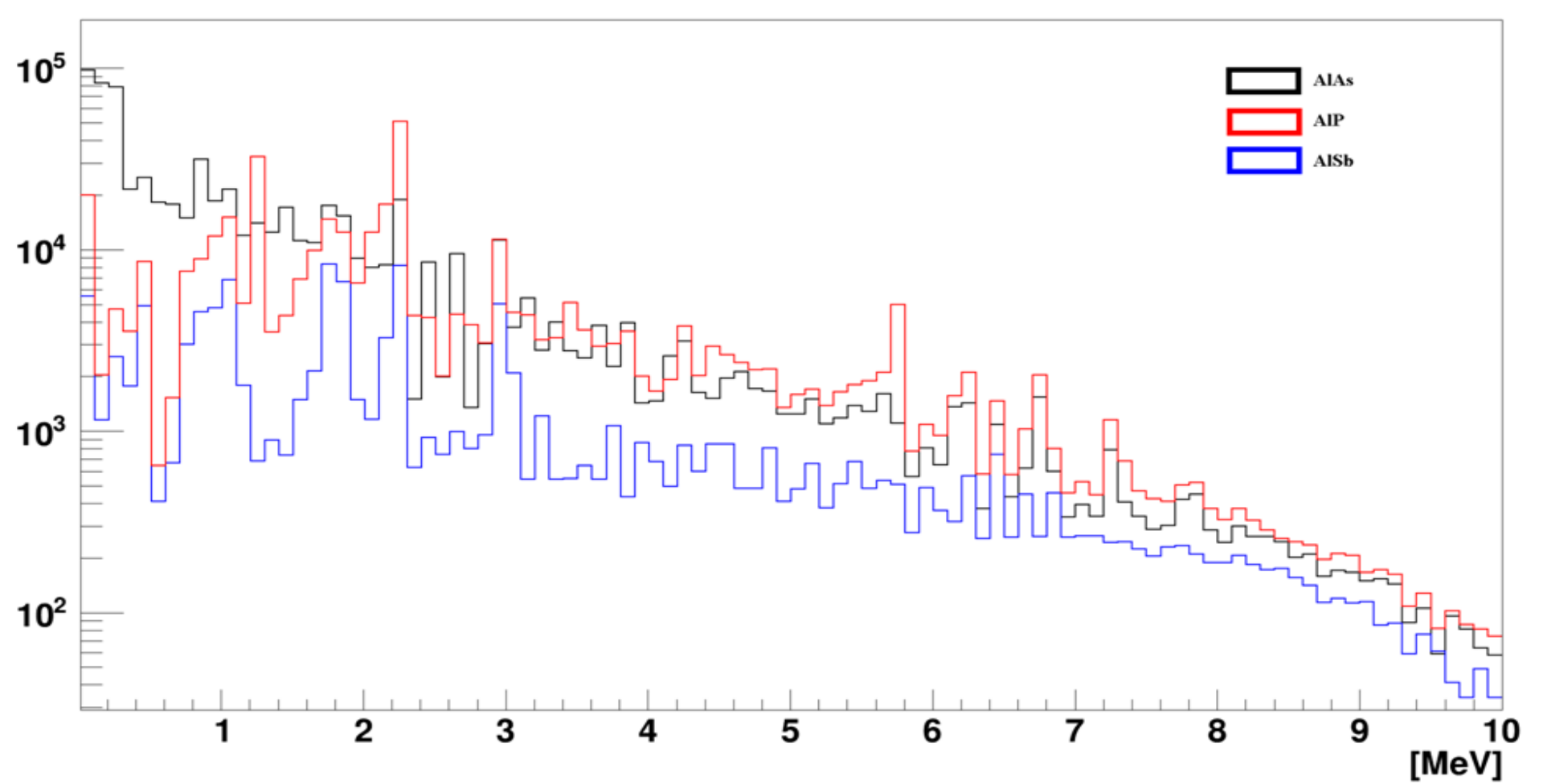

Потери на кинетическую энергию в материалах AlAs, AlP, AlSb при облучении нейтронным потоком энергией 14 МэВ

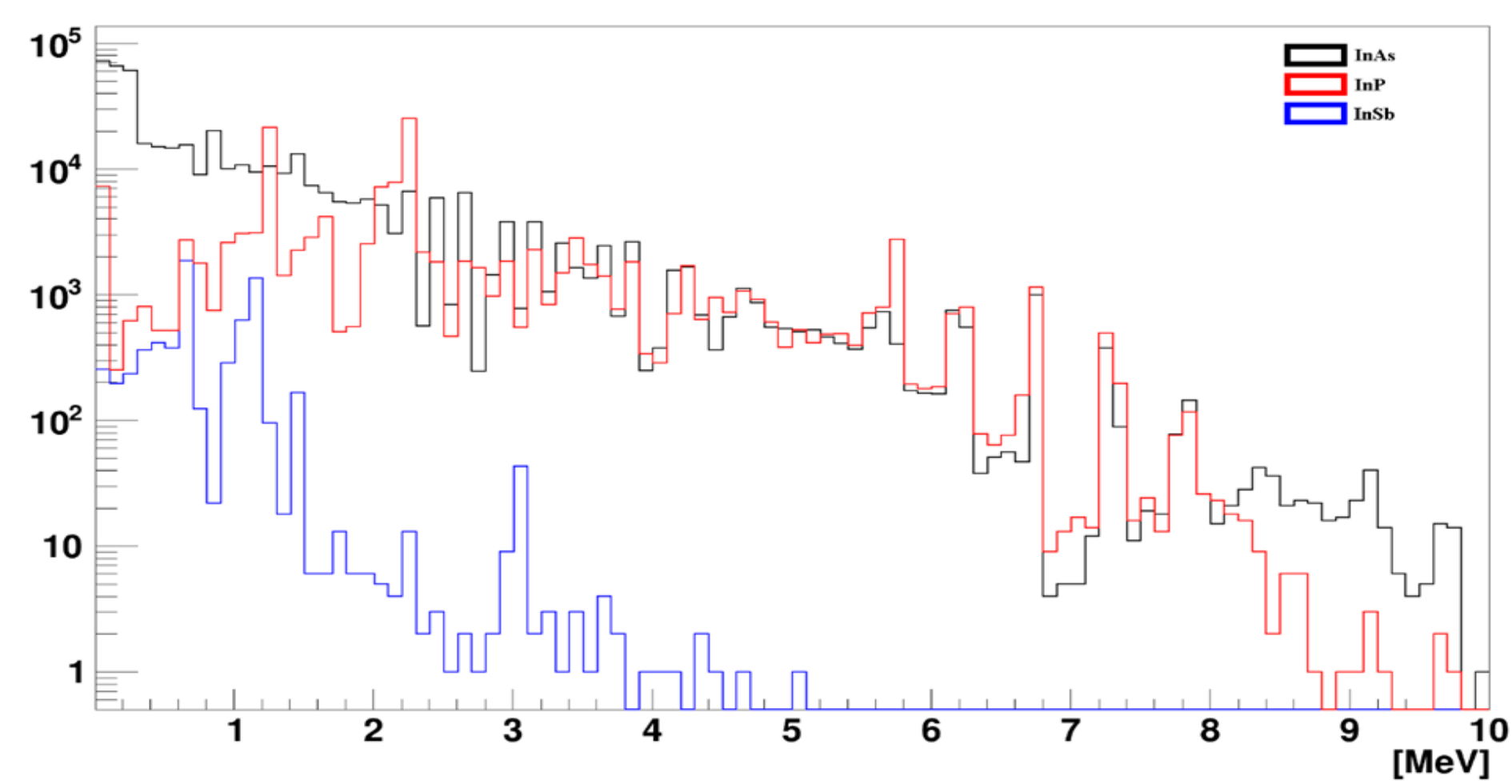

Потери на кинетическую энергию в материалах InAs, InP, InSb при облучении нейтронным потоком энергией 14 МэВ

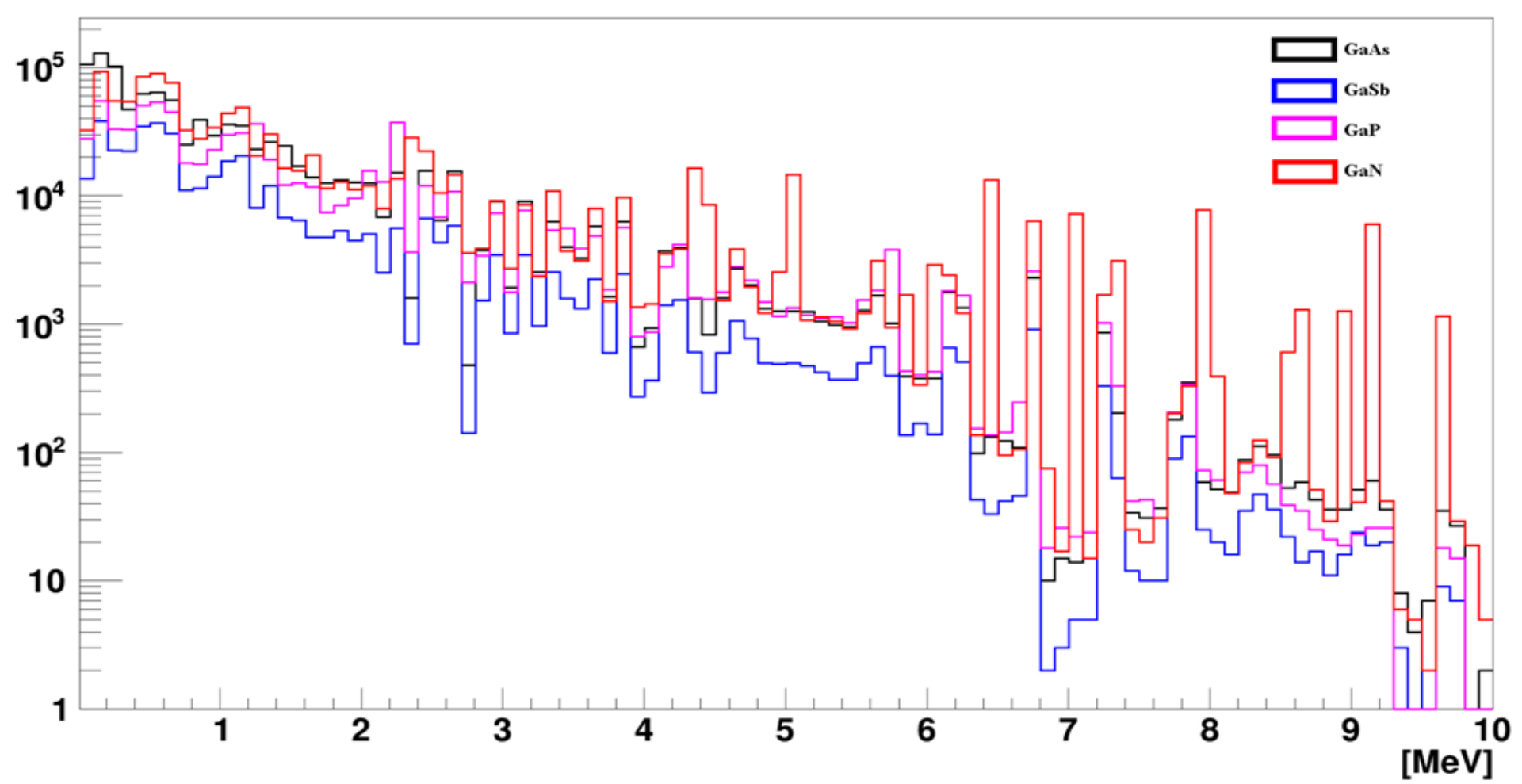

Потери на кинетическую энергию в материалах GaAs, GaP, GaSb, GaN при облучении нейтронным потоком энергией 14 МэВ

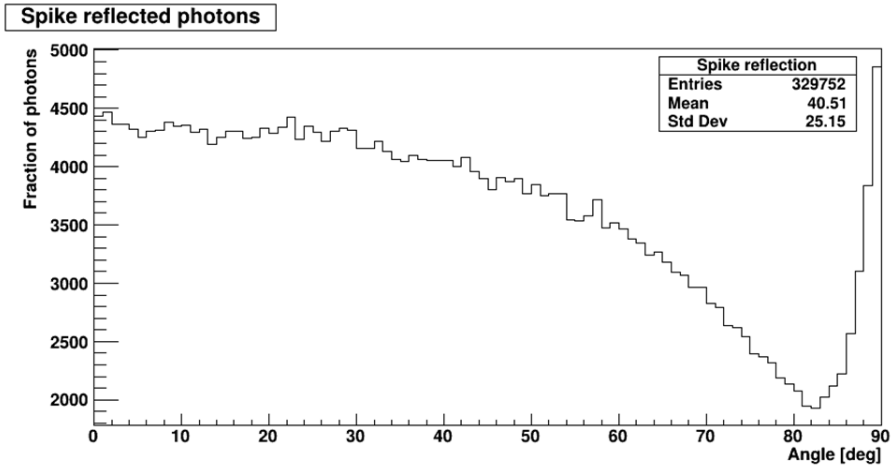

Доля отражённых материалом фотонов до облучения

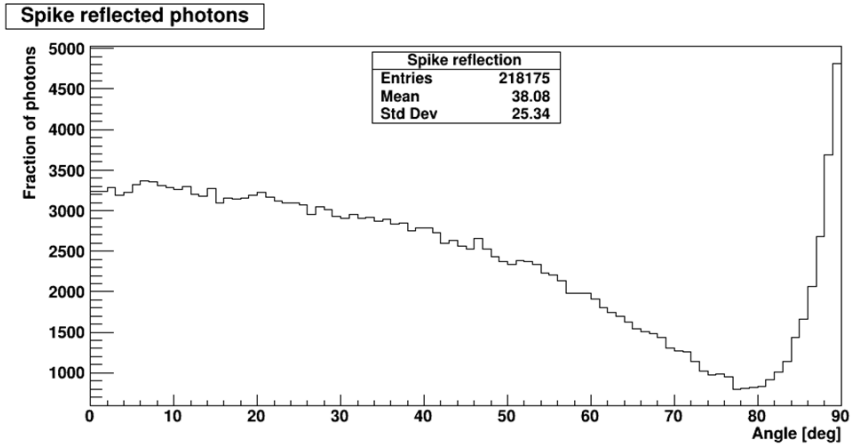

Доля отражённых материалом фотонов после облучения